Neural Neighborhood Encoding for Classification

Kaushik Sinha
Wichita State University, USA
kaushik.sinha@wichita.edu

Parikshit Ram
IBM Research, USA
p.ram@gatech.edu

August 21, 2020

Abstract

Inspired by the fruit-fly olfactory circuit, the Fly Bloom Filter [Dasgupta et al., 2018] is able to efficiently summarize the data with a single pass and has been used for novelty detection. We propose a new classifier (for binary and multi-class classification) that effectively encodes the different local neighborhoods for each class with a per-class Fly Bloom Filter. The inference on test data requires an efficient `FlyHash` [Dasgupta et al., 2017] operation followed by a high-dimensional, but *sparse*, dot product with the per-class Bloom Filters. The learning is trivially parallelizable. On the theoretical side, we establish conditions under which the prediction of our proposed classifier on any test example agrees with the prediction of the nearest neighbor classifier with high probability. We extensively evaluate our proposed scheme with over 50 data sets of varied data dimensionality to demonstrate that the predictive performance of our proposed neuroscience inspired classifier is competitive the the nearest-neighbor classifiers and other single-pass classifiers.

1 Introduction: Neurally inspired data structure

Neural circuits in the fruit-fly appear to assess the novelty of an odor in a two step process. Any odor is first assigned a "tag" that corresponds to a small set of Kenyon Cells (KC) that get activated by the odor. Dasgupta et al. [2017] interpret this tag generation process as a hashing scheme, termed `FlyHash`, where the tag/hash is effectively a very sparse point a high dimensional space (2000 dimensions with $\sim 95\%$ sparsity). The tag (or rather a subset of it) serves as input to a specific mushroom body output neuron (MBON), the MBON-$\alpha'3$, where the response of this neuron to the odor hash encodes the novelty of an odor. Dasgupta et al. [2018] "interpret the KC→MBON-$\alpha'3$ synapses as a Bloom Filter" that effectively "stores" all odors previously exposed to the fruit-fly. This *Fly Bloom Filter* (`FBF`) generates continuous valued, distance and time sensitive novelty scores that have been empirically shown to be highly correlated to the ground-truth novelty scores relative to other Bloom Filter-based novelty scores for both neural activity data sets (odors and faces) and vision data sets (MNIST and SIFT). Theoretically, bounds on the expected novelty scores of similar and dissimilar points have been established for binary and exponentially distributed data.

In this paper, we propose a **simple** extension of `FBF` to binary and multi-class classification, where we summarize each class with its own `FBF` and utilize the *familiarity* scores (inverse novelty scores) from each class to label any test point. We theoretically study why this simple idea works, and empirically demonstrate that the simplicity does not preclude utility. Specifically, we present

▶ A novel `FBF` based classifier (`FBFC`) that can be learned in an *embarrassingly parallelized* fashion with a *single pass* of the training set, *provide insights* into the problem structure, and can be inferred from with an *efficient* `FlyHash` [Dasgupta et al., 2017] followed by a *sparse* dot-product.

▶ A theoretical examination of the proposed scheme, establishing conditions under which `FBFC` *agrees* with the nearest-neighbor classifier.

▶ A thorough empirical comparison of `FBFC` to k-nearest-neighbor (k-NNC) and other standard classifiers on over 50 data sets from different domains.

▶ A demonstration of the scaling of the parallelized `FBFC` training process.

▶ We present how the `FBFC` can be used to interpret similarities between different classes in classification problem.

The paper is organized as follows: We discuss related work in Section 2. We detail our proposed algorithm in Section 3 and analyze its theoretical properties in Section 4. We evaluate the empirical performance of `FBFC` against baselines in Section 5 and conclude with a discussion in Section 6.

2   Related work

Neuroscience inspired techniques are now widely accepted in artificial intelligence to great success [Hassabis et al., 2017], especially in the field of deep learning in the form of convolutional neural networks [Kavukcuoglu et al., 2010, Krizhevsky et al., 2012], dropout [Hinton et al., 2012] and attention mechanisms [Larochelle and Hinton, 2010, Mnih et al., 2014] to name a few. Much like most machine learning methods, deep learning relies on loss-gradient based training in most cases. In contrast, our proposed `FBFC` learning does not explicitly minimize any "loss" function. Moreover, rather than learning a representation for the points that facilitates classification/regression, the `FBFC` learns a representation for entire classes, allowing test points to be compared to classes for computing familiarity scores.

Given the correlation between a point x's `FBF` novelty score to its minimum distance from the set that the `FBF` summarizes [Dasgupta et al., 2018], our proposed neuroscience inspired `FBFC` is perhaps closest to the nonparametric k-nearest-neighbor classifier (`k-NNC`). Vanilla `k-NNC` does not have an explicit loss or a training phase given a measure of similarity; all the computation is shifted to inference. `FBFC` does have an explicit training phase, but requires only a single pass of the training data – once a point is processed into the `FBF`, it can be discarded, making `FBFC` suitable for streaming data.

On a very high level, this is similar to cluster-based `k-NNC` where class specific training data (data with same labels) is summarized as (multiple) cluster centers and used as a reduced training set on which `k-NNC` is applied. A variety of methods exists in literature that adopt this simple idea of data reduction [Zhou et al., 2010, Parvin et al., 2012, Oigiaroglou and Evangelidis, 2013, 2016, Gallego et al., 2018, Gou et al., 2019]. These algorithms are designed with the goal of reducing the high computational & storage requirements of `k-NNC`. Orthogonally, various data structures have been utilized to accelerate the nearest-neighbor search in `k-NNC` inference representing the data as an index such as space-partitioning trees Omohundro [1989], Beygelzimer et al. [2006], Dasgupta and Sinha [2015], Ram and Sinha [2019] and hash tables generated by *locality-sensitive* hashes Gionis et al. [1999], Andoni and Indyk [2008].

The closely related locality-sensitive Bloom filter (LSBF) Kirsch and Mitzenmacher [2006], Hua et al. [2012] also summarizes the data similar to `FBF`, relying on distance preserving random projection Vempala [2004] to lower dimensionalities followed by quantizing the projected vector to an integer. Under this scheme, two inputs reset the same bit in the filter if they are assigned the exact same projected vector. Performance of LSBF heavily depends on the choice of hyperparameters that control the projection dimensionality and the data-independent quantization scheme. `FBF` has been shown to be empirically outperform LSBF for novelty detection.

Multinomial regression with linear models and multi-layered perceptron can also be viewed as learning a set of weight vectors corresponding to each class, with the inner product of the test point with these vectors driving the class assignment.

3   `FlyHash` Bloom Filter Classifier (`FBFC`)

The basic building block of our proposed algorithm is a fruit-fly olfactory circuit inspired `FlyHash` function, first introduced by Dasgupta et al. [2017]. Here we consider the binarized `FlyHash` [Dasgupta et al., 2018]. For $x \in \mathbb{R}^d$, the `FlyHash` function $h: \mathbb{R}^d \to \{0, 1\}^m$ is defined as,

$$h(x) = \Gamma_\rho(M_m^s x), \tag{1}$$
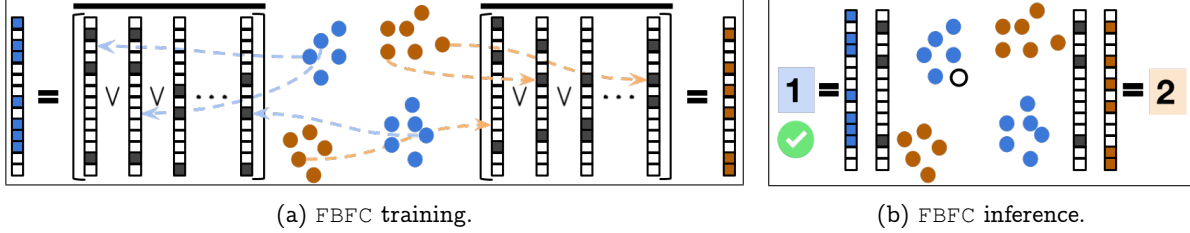
(a) FBFC training.   (b) FBFC inference.

Figure 1: Visual depiction of FBFC training (Algorithm 1) and inference (Equation (3)) for FBFC. Colored circles correspond to the labeled training set. In Figure 1a, the high dimensional sparse FlyHashes for the points (stacked ■ & □) in each class are used to generate the per-class FBF (NOT $\overline{(\cdot)}$ of the ORs $\vee$ of the hashes as per Equation (2)). The ◯ in Figure 1b is the unlabeled point we infer on based on the dot-product of its FlyHash with each of the per-class FBFs (eliding the denominator in Equation (3)). *Please view in color.*

where $M_m^s \in \{0,1\}^{m \times d}$ is the randomized sparse lifting binary matrix with $s \ll d$ nonzero entries in each row, and $\Gamma_\rho \colon \mathbb{R}^m \to \{0,1\}^m$ is the winner-take-all function converting a vector in $\mathbb{R}^m$ to one in $\{0,1\}^m$ by setting the highest $\rho \ll m$ elements to 1 and the rest to zero[1]. Unlike random projection Vempala [2004] which decreases data dimensionality after projection, FlyHash is an upward projection which increases data dimensionality ($m \gg d$). The hyper-parameters for FlyHash are (i) the projected dimensionality $m \in \mathbb{N}$, (ii) projection matrix nonzero count per row $s \in \mathbb{N}$, and (iii) the number of nonzeros (NNZ) $\rho \in \mathbb{N}$ in the FlyHash. The run time for FlyHash is $O(ms + m\log\rho)$. The FlyHash function can also be viewed as a maximum inner product search problem [Ram and Gray, 2012, Shrivastava and Li, 2014] where we seek the ρ rows in M_m^s with the highest inner-product to x and sped up using fast algorithms.

Using FlyHash as an algorithmic building block, Dasgupta et al. [2018] construct a FBF to succinctly summarize the data, and use it to effectively solve the unsupervised learning task of novelty detection. Here we extend the use of FBF to classification, an instance of supervised learning. Specifically, we use FBF to summarize each class separately – the per-class FBF encodes the local neighborhoods of each class, and the high dimensional sparse nature of FlyHash (and consequently FBF) summarizes classes with multi-modal distributions while mitigating overlap between the FBFs of other classes.

FBFC training. Let $w_i \in \{0,1\}^m$ be the FBF for any class $i \in [L] = \{1, 2, \ldots, L\}$, with w_i initialized to $\mathbf{1}_m \in \{0,1\}^m$, the all one vector. For any point $x \in \mathbb{R}^d$ with label $y = i$ in the training set $S \subset \mathbb{R}^d \times [L]$, w_i is updated with the FlyHash $h(x)$ as follows – the bit positions of w_i corresponding to the nonzero bit positions of $h(x)$ are set to zero, represented as $w_i \leftarrow (w_i \oplus h(x)) \wedge w_i = w_i \wedge \overline{h(x)}$, where $\oplus, \wedge$ and $\overline{(\cdot)}$ are the XOR, AND and NOT operators respectively. Starting with $w_i = \mathbf{1}_m$, the updates for any two examples $(x_1, y_1), (x_2, y_2) \in S$ with $y_1 = y_2 = i$ can be succinctly written as $w_i \leftarrow \overline{\mathbf{1}_m \vee h(x_1) \vee h(x_2)}$ with the application of De Morgan's law, with $\vee$ as OR. We can now condense the FBF construction for a class $i \in [L]$ to

$$w_i = \overline{\mathbf{1}_m \bigvee_{(x,y) \in S \colon y=i} h(x)} = \overline{\bigvee_{(x,y) \in S \colon y=i} h(x)} = \mathbf{1}_m \bigwedge_{(x,y) \in S \colon y=i} \overline{h(x)} = \bigwedge_{(x,y) \in S \colon y=i} \overline{h(x)}. \tag{2}$$

This new interpretation makes the FBF construction trivially parallelizable – w_i for each $i \in [L]$ can be computed either by a series of commutative ORs followed by a NOT at the end or by a series of commutative ANDs, and the process is order-independent. The L per-class FBFs (and the lifting matrix M_m^s) constitute our proposed *FBFC*. Algorithm 1 (TrainFBFC) presents the FBFC training, and Figure 1a visualizes the process for a toy example.

FBFC inference. For a point x, we compute the per-class novelty scores $f_i(x) \in [0,1], i \in [L]$ and the

---

[1] FlyHash Dasgupta et al. [2017] leaves the highest ρ elements as is and sets the rest to zero, but requires each $x \in \mathbb{R}^d$ to be mean-centered ($\sum_{i=1}^d x_i = 0$). FBF needs a binarized FlyHash [Dasgupta et al., 2018], where mean-centering is redundant.

3

predicted label as:

$$f_i(x) = \left(w_i^\top h(x)\right)/\rho, \quad \hat{y} = \arg\min_{i \in [L]} f_i(x) \tag{3}$$

A high $f_i(x)$ indicates that majority of the training examples with label i are very different from x. A small value of $f_i(x)$ indicates the existence of at least one training example with label i similar to x. The predicted label for x is simply the class with the smallest $f_i(x)$ (breaking ties randomly). This is visualized in Figure 1b. The per-class $f_i(x), i \in [L]$ can be converted into class probabilities with a soft-max operation.

Computational complexities. FBFC training time with n points is $O(nms + nm\log\rho + n\rho)$ for the n FlyHash operations, followed by n ORs with the class-specific FBFs. The commutative OR operator allows us to chunk n points across T threads for parallel processing of groups of size n/T – in a shared memory setting, all threads operate on the same set of per-class FBFs, resulting in a $O\left(\frac{n}{T}\left(ms + m\log\rho + \rho\right)\right)$ runtime, demonstrating linear scaling with T. In distributed memory setting, each process operates its own set of FBFs that are finally *all-reduced* in additional $O(mL\log T)$ time. Memory overhead for training with a batch of n' training point is $O(ms + n'm + mL)$. The batch size can be as small as 1, implying a minimum memory overhead during training of $O(m(s+L))$. If T threads are processing batches of size n' each, the memory overhead increases linearly with T. FBFC

Algorithm 1: FBFC training with training set $S \subset \mathbb{R}^d \times [L]$, projected dimensionality $m \in \mathbb{N}$, NNZ for each row in the projection matrix $s \ll d$, NNZ in the FlyHash $\rho \ll m$.

1 **Function TrainFBFC:**
    $(S, m, \rho, s) \rightarrow (M_m^s, \{w_i, i \in [L]\})$
2   Initialize $w_1, \ldots, w_L \leftarrow \mathbf{1}_m \in \{0,1\}^m$
3     $M_m^s \in \{0,1\}^{m \times d}$ // s NNZ per row
4   **for** $(x, y) \in S$ **do**
5         $h(x) \leftarrow \Gamma_\rho(M_m^s x)$
6         $w_y \leftarrow w_y \bigwedge \overline{h(x)}$
7   **end**
8   **return** $(M_m^s, \{w_i, i \in [L]\})$
9 **end**

---

inference takes $O(ms + m\log\rho + L\rho)$ per point. However, the inference problem $\min_{i \in L} w_i^\top h(x)$ can be reduced to a maximum inner product search problem [Ram and Gray, 2012, Shrivastava and Li, 2014] and solved in time sublinear in L for large L.

Inter-class similarities. Given the per-class FBFs $w_i, i \in [L]$, we propose the cosine similarity s_{ij} between the FBF pair (w_i, w_j) as a similarity score between classes i and j to quantify the hardness of differentiating these classes, and provides an insight into the structure of the classification problem.

Non-binary FBF. In our binary FBF design, for any test point x and any $i \in [L]$, let $A_x = \{j : (h(x))_j = 1\}$ be the nonzero coordinates in $h(x)$. Each coordinate of A_x contributes in deciding the value of $f_i(x)$. For any $j \in A_x$, it is possible that a single training example x' from class i sets the contribution of the jth coordinate to zero in the computation of $f_i(x)$ – it is only required that $h((x'))_j = 1$; since h is randomized, there is always a nonzero probability of this event. Also, for any $j, k \in A_x, j \neq k$, if $w_{ij} = w_{ik} = 0$ (the jth and k^{th} element in the FBF for class i), coordinates j and k are indistinguishable in terms of their contribution to $f_i(x)$. To address these limitations, we present a modified FBF design which aims to capture neighborhoods and distribution information more effectively, by allowing coordinates of w_i to take value in $[0,1]$. In this design, for any fixed $c \in (0,1]$, the jth coordinate of w_i is set as follows, with $c = 1$ corresponding to binary FBF:

$$w_{ij} = (1-c)^{\left|\{(x,y) \in S : y=i \text{ and } (h(x))_j = 1\}\right|}, \tag{4}$$

The label for a test point $x \in \mathbb{R}^d$ is still computed as $\hat{y} = \arg\min_{i \in [L]} w_i^\top h(x)$. We term this form of the Fly Bloom Filter as FBF* and the corresponding classifier as FBFC*. For any i, j, since w_{ij} is computed by counting the number of examples $(x', y') \in S$ satisfying $y' = i$ and $(h(x'))_j = 1$, and raising this count to the power of $(1-c)$, FBF* is still equally parallelizable as the binary FBF– the OR aggregation followed by a NOT is now instead a (sparse) summation over the FlyHashes, followed by an exponentiation of $(1-c)$. The exponential decay in equation (4) allows w_{ij} to be determined by a local neighborhood of size dependent on c. We discuss this further in Supplement S1.

4 Theoretical analysis

In this section we present theoretical analysis of FBFC, identifying conditions under with FBFC agrees with the nearest-neighbor classifier 1-NNC. First we describe the general setup and present our generic analysis when certain abstract conditions are satisfied. Then we consider two special cases that are different instantiations of this generic result. All proofs are deferred to Supplement S2.

4.1 Preliminaries

We denote a single row of a projection matrix M_m^s by $\theta \in \{0, 1\}^d$ drawn i.i.d. from Q, the uniform distribution over all vectors in $\{0, 1\}^d$ with exactly s ones, satisfying $s \ll d$. For ease of notation, we use M instead of M_m^s and we use an alternate formulation of the winner-take-all strategy as suggested in Dasgupta et al. [2018], where for any $x \in \mathbb{R}^d, \tau_x$ is a threshold that sets largest ρ entries of Mx to one (and the rest to zero) in expectation. Specifically, for a given $x \in \mathbb{R}^d$ and for any fraction $0 < f < 1$, we define $\tau_x(f)$ to be the top f-fractile value of the distribution $\theta^\top x$, where $\theta \sim Q$:

$$\tau_x(f) = \sup\{v : \Pr_{\theta \sim Q}(\theta^\top x \geq v) \geq f\} \tag{5}$$

We note that for any $0 < f < 1$, $\Pr_{\theta \sim Q}(\theta^\top x \geq \tau_x(f)) \approx f$, where the approximation arises from possible discretization issues. For convenience, henceforth we will assume that this is an equality:

$$\Pr_{\theta \sim Q}(\theta^\top x \geq \tau_x(f)) = f \tag{6}$$

For any two $x, x' \in \mathbb{R}^d$, we define: $q(x, x') = \Pr_{\theta \sim Q}(\theta^\top x' \geq \tau_{x'}(\rho/m) \mid \theta^\top x \geq \tau_x(\rho/m))$. This can be interpreted as follows: with $h(x), h(x')$ as the FlyHashes of x and x', respectively, $q(x, x')$ is the probability that $(h(x'))_j = 1$ given that $(h(x))_j = 1$, for any specific j.

We analyze classification performance of FBFC trained on a training set $S = \{(x_i, y_i)\}_{i=1}^{n_0+n_1} \subset \mathcal{X} \times \{0, 1\}$, where $S = S^1 \cup S^0$, S^0 is a subset of S having label 0, and S^1 is a subset of S having label 1, satisfying $|S^0| = n_0, |S^1| = n_1$ and $n = \max\{n_0, n_1\}$. For appropriate choice of m, let $w_0, w_1 \in \{0, 1\}^m$ be the FBFs constructed using S^0 and S_1 respectively.

4.2 Connection to 1-NNC

Without loss of generality, for any test example $x \in \mathcal{X}$, assume that its nearest neighbor from S has class label 1. Then 1-NNC will predict x's class label to be 1. With $h(x)$ as the FlyHash of x (equation 1), if we are able to show that $\mathbb{E}_M(w_1^\top h(x)) < \mathbb{E}_M(w_0^\top h(x))$ then FBFC will predict, in expectation, x's label to be 1. The following lemma quantifies the expectation of class specific novelty scores and their upper and lower bounds.

Lemma 1. *Fix any* $x \in \mathbb{R}^d$ *and let* $h(x) \in \{0, 1\}^m$ *be its FlyHash using equation 1. Let* $x_{NN}^i = \arg\min_{(x', y') \in S^i} \|x - x'\|$ *for* $i \in \{0, 1\}$, *where* $\|\cdot\|$ *is any distance metric. Let* $A_{S^1} = \{\theta : \cap_{(x', y') \in S^1} \theta^\top x' < \tau_{x'}(\rho/m)\}$ *and* $A_{S^0} = \{\theta : \cap_{(x', y') \in S^0} \theta^\top x' < \tau_{x'}(\rho/m)\}$. *Then the following holds, where the expectation is taken over the random choice of projection matrix* M.
(i) $\mathbb{E}_M(\frac{w_1^\top h(x)}{\rho}) = \Pr_{\theta \sim Q}(A_{S^1} | \theta^\top x \geq \tau_x(\frac{\rho}{m}))$, *(ii)* $\mathbb{E}_M(\frac{w_0^\top h(x)}{\rho}) = \Pr_{\theta \sim Q}(A_{S^0} | \theta^\top x \geq \tau_x(\frac{\rho}{m}))$
(iii) $\mathbb{E}_M(\frac{w_1^\top h(x)}{\rho}) \geq 1 - \sum_{x' \in S^1} q(x, x')$, *(iv)* $\mathbb{E}_M(\frac{w_1^\top h(x)}{\rho}) \leq 1 - q(x, x_{NN}^1)$
(v) $\mathbb{E}_M(\frac{w_0^\top h(x)}{\rho}) \geq 1 - \sum_{x' \in S^0} q(x, x')$, *(vi)* $\mathbb{E}_M(\frac{w_0^\top h(x)}{\rho}) \leq 1 - q(x, x_{NN}^0)$

This immediately provides us a sufficient condition for FBFC to agree with 1-NNC on any test point x in expectation – the upper bound of $\mathbb{E}_M(w_1^\top h(x))$ should be strictly smaller than lower bound of $\mathbb{E}_M(w_0^\top h(x))$.

Theorem 2. *Fix any* $\delta \in (0, 1)$, $s \ll d$, *and* $\rho \ll m$. *Given a training set* S *as described above and a test example* $x \in \mathcal{X}$, *let* x_{NN} *be its closest point from* S *measured using* ℓ_p *metric for an appropriate*

choice of p. *If (i)* $\rho = \Omega(\log(1/\delta))$, *(ii)* $\|x - x_{NN}\|_p = O(1/s)$, *and (iii)* $m = \Omega(n\rho)$, *then under mild conditions, with probability at least* $1 - \delta$ *(over the random choice of projection matrix* M*), prediction of* `FBFC` *on* x *agrees with the prediction of 1-NN classifier on* x.

Proof (sketch). If either the structure of $\mathcal{X}$ allows us to choose a threshold τ_x that is identical for any $x \in \mathcal{X}$, resulting in a closed form solution for the quantity $q(x, x')$ for any $x, x' \in \mathcal{X}$, or the distributional assumption on $\mathcal{X}$ sets the quantity $\mathbb{E}_x q(x, x')$ to be identical for all $x' \in S$, then all the three conditions mentioned in theorem are satisfied. This property, in conjunction with Lemma 1, yields the desired result in expectation under mild conditions. The high probability result then follows using standard concentration bounds.

Multi-class classification. The above results can be extended to multi-class classification problem involving L classes in a straight forward manner by applying concentration result to each of the $\left((w_i^\top h(x))/\rho \right)$, for $i \in [L]$, and using a union bound (see Supplement S2.4).

Note that the `FBF` guarantees for novelty detection are limited to two special cases: (i) examples with binary feature vectors containing fixed number of ones, and (ii) examples sampled from a permutation invariant distribution Dasgupta et al. [2018]. We extend this analysis with these two cases to provide guarantees for `FBFC` in multi-class classification, which is a distinct learning problem from novelty detection.

4.3 Special case I: Binary data

In this section we consider a special case where examples from each class have binary feature vectors with fixed number of ones. In particular, let $\mathcal{X} = \mathcal{X}_b = \{x \in \{0, 1\}^d : |x|_1 = b < d\}$.

Theorem 3. *Let S be a training set as given above. Fix any $\delta \in (0, 1)$, and set $\rho \geq \frac{12}{\mu} \ln(4/\delta)$, $m \geq (d/b)n\rho$, and $s = \log_{d/b}(m/\rho)$, where $\mu = \min\left\{\mathbb{E}_M\left((w_0^\top h(x))/\rho\right), \mathbb{E}_M\left((w_1^\top h(x))/\rho\right)\right\}$ and $h(x)$ is the `FlyHash` (eq. (1)). For a test point $x \in \mathcal{X}$, let its closest point from S measured using ℓ_1 metric be x_{NN}, having label $y_{NN} \in \{0, 1\}$, satisfies, (i) $\|x - x_{NN}\|_1 \leq 2b(1 - b/d)/3s$, and (ii) $\|x - x_i\|_1 \geq 2b(1 - b/d)$ for all $(x_i, y_i) \in S$, with $y_i \neq y_{NN}$. Let $w_0, w_1 \in \{0, 1\}^m$ be the `FBF`s constructed using S^0 and S^1 respectively. Then, with probability at least $1 - \delta$ (over the random choice of projection matrix M), `FBFC` prediction on x agrees with the $1-NNC$ prediction on x.*

Here $s = O(\log n)$, which is the same logarithmic dependence that was also established in Dasgupta et al. [2018].

4.4 Special Case II: Permutation invariant distribution in $\mathbb{R}^d$

Here we show that, for *permutation invariant* distributions, `FBFC` agrees with $1-NNC$ in $\mathbb{R}^d$ with high probability. Permutation invariant distribution in the `FBF` context was introduced in Dasgupta et al. [2018] and defined as a distribution P over $\mathbb{R}^d$ permutation σ of $\{1, 2, \ldots, d\}$ and any $x = (x_1, \ldots, x_d) \in \mathbb{R}^d$, $P(x_1, \ldots, x_d) = P(x_{\sigma(1)}, \ldots, x_{\sigma(d)})$. Precisely, we show

Theorem 4. *Let S be a training set as given above. Fix any $\delta \in (0, 1)$, $s \ll d$, and set $\rho \geq \frac{48}{\mu} \ln(8/\delta)$ and $m \geq 14n\rho/\delta$, where $\mu = \min\left\{\mathbb{E}_M\left((w_0^\top h(x))/\rho\right), \mathbb{E}_M\left((w_1^\top h(x))/\rho\right)\right\}$, $h(x)$ is the `FlyHash` (eq. (1)), and $w_0, w_1 \in \{0, 1\}^m$ are the `FBF`s constructed using S^0 and S^1 respectively. For a test point $x \in \mathbb{R}^d$, sampled from a permutation invariant distribution, let x_{NN} be its nearest neighbor from S measured using ℓ_∞ metric, which satisfies $\|x - x_{NN}\|_\infty \leq \Delta/s$, where $\Delta = \frac{1}{2}\left(\tau_x(2\rho/m) - \tau_x(\rho/m)\right)$ and has label $y_{NN} \in \{0, 1\}$. Then, with probability at least $1 - \delta$ (over the random choice of projection matrix M), `FBFC` prediction on x agrees with $1-NNC$ prediction on x.*

Towards $\mathbb{R}^d$. The structure of the binary and permutation-invariant distributions allow us to get these novel, yet limited, result. Similar results for general $\mathbb{R}^d$ are more challenging and non-trivial – for any $x, x' \in \mathbb{R}^d, x \neq x'$, the thresholds τ_x and $\tau_{x'}$ will be different and a closed form solution for $q(x, x')$ may not

exist, and we need to find explicit bounds for this quantity. Our hypothesis is that we will need various data dependent assumptions, including smoothness of conditional probability function and Tsybakov's margin conditions [Tsybakov, 2004, Audibert and Tsybakov, 2007], to get a similar result for $\mathbb{R}^d$.

5 Empirical evaluations

In this section, we evaluate the empirical performance of FBFC. First, we evaluate the dependence of FBFC on its hyper-parameteres. Then, we compare FBFC to other classifiers that can be trained in a single pass on (i) synthetic data, (ii) OpenML (binary & multi-class) classification data sets [Van Rijn et al., 2013], and (iii) 4 popular vision data sets – MNIST, FASHION-MNIST, CIFAR10, CIFAR100. Finally, we study the computational scaling of the parallelized FBFC training and present some problem insights generated by a trained FBFC. The details on the implementation and compute resources are in Supplement S3.

5.1 Dependence on hyper-parameters

We study the effect of the different FBFC hyper-parameters: (i) the FlyHash dimension m, (ii) the NNZ per-row $s \ll d$ in M_m^s, (iii) the NNZ ρ in the FlyHash, and (iv) the FBF decay rate c. We consider 6 OpenML data sets (see Table S1 in Supplement S3 for data details). For every hyper-parameter setting, we compute the 10-fold cross-validated classification accuracy ($1-$ misclassification rate). We vary each hyper-parameter while fixing the others. The results for each of the hyper-parameters and data sets are presented in Figures S1 & S2 in Supplement S3.1.

The results indicate that, for fixed ρ, increasing m usually improves FBFC performance up to a point. FBFC performance is not affected by s for the high dimensional sets; for the lower dimensional sets ($d < 20$), the performance improves with increasing s till around $s \approx 10$, after which, the performance degrades. Increase in ρ improves FBFC performance for fixed values of m and other hyper-parameters. The FBFC performance is not affected much by the value of the decay rate when $c < 1$, but there is a significant drop in performance as we move from $c < 1$ (non-binary FBF) to $c = 1$ (binary FBF), indicating the advantage of our novel non-binary FBF; this behavior is pretty consistent and obvious across all data sets. See Supplement S3.1 for further details and discussion.

5.2 Comparison to baselines

We compare our proposed FBFC to various baselines. Given the significant difference between FBFC with $c = 1$ (binary Bloom Filter) and FBFC with $c < 1$, we consider both cases, with FBFC* explicitly denoting $c < 1$. We evaluate the proposed schemes and all the baselines relative to the k-nearest-neighbor classifier (k-NNC). We consider a variety of baselines, including ones that can be trained in a single pass of the training data (similar to FBFC):

▶ **k-NNC:** This is the primary baseline. We tune over the neighborhood size $k \in [1, 64]$.

▶ **CC1:** We consider classification based on a single prototype per class – the geometric center of the class, computed with a single pass of the training set.

▶ **CC:** This generalizes CC1 where we utilize multiple prototypes per class – a test point is assigned the label of its closest prototype. The per-class prototypes are obtained by k'-means clustering. We tune over the number of clusters per-class $k' \in [1, 64]$. This is *not single pass*.

▶ **SBFC:** We utilize SimHash [Charikar, 2002] based LSBF for each class in place of FBF to get the SimHash Bloom Filter classifier (SBFC). We consider this to demonstrate the need for the high level of sparsity in FlyHash; SimHash is not inherently as sparse. We tune over the SimHash projected dimension m, considering $m < d$ (traditional) and $m > d$ (as in FlyHash). For the same m, SimHash is more costly than FlyHash, involving a dense matrix-vector product instead of a sparse matrix-vector one.

▶ **LR.** We consider logistic regression trained for a single epoch with a stochastic algorithm and tune over 960 hyper-parameter configurations for each data set.
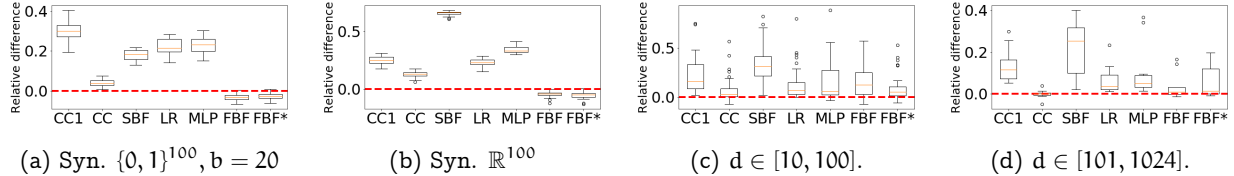
| (a) Syn. $\{0,1\}^{100}, b = 20$ | (b) Syn. $\mathbb{R}^{100}$ | (c) $d \in [10, 100]$. | (d) $d \in [101, 1024]$. |

Figure 2: Performance of FBFC/FBFC* and baselines relative to the k−NNC performance on *synthetic* (2a & 2b) and *OpenML* data (2c & 2d). The 10-fold cross-validated accuracy is considered for each of the data sets. The box-plots correspond to performance relative to k−NNC (*lower is better*) aggregated over multiple data sets (see text for details). The red dashed line denotes k−NNC performance.

▶ **MLPC.** We consider a multi-layer perceptron trained for a single epoch with the "Adam" solver [Kingma and Ba, 2014] and tune over 288 hyper-parameter configurations for each data set.

The complete details of the baselines and their hyper-parameters are in Supplement S3.2.

FBFC hyper-parameters. For a data set with d dimensions, we tune across 60 hyper-parameter settings in the following ranges: $m \in [2d, 2048d]$, $s \in (0.0, 0.5d]$, $\rho \in [8, 256]$, and $c \in [0.2, 1]$, with $c = 1$ as binary FBFC. We use this hyper-parameter search space for all experiments, except for the vision sets, where we use $m \in [2d, 1024d]$.

Evaluation metric. For all methods (baselines and FBFC), we compute the relative performance on each data set as $(1 − a_M/a_k)$ where a_k is the best 10-fold cross-validated classification accuracy achieved by k−NNC and a_M is the best 10-fold cross-validated classification accuracy obtained by candidate method M across different hyper-parameters. k−NNC has a relative performance of 0.

5.2.1 Synthetic data

We begin with binary synthetic data of the form considered in our theoretical results – points $x \in \{0,1\}^d$ with $|x| = b < d$. We then consider synthetic data in $\mathbb{R}^d$. We cover different values of d and b and create a 5-class classification sets with 3 modes per class. For each value of d (and b), we create 30 data sets with 1000 points each. The aggregate performance of all baselines (aggregated across all instantiations of $d = 100$ ($b = 20$)) is presented in Figures 2a and 2b. More results on synthetic data sets with different values of d (and b) are presented is Supplement S3.3.

The results indicate that FBFC and FBFC* are able to match k−NNC performance significantly better than all other single pass baselines. The binary FBFC matches the performance of FBFC* in $\mathbb{R}^d$, but lags behind on the lower dimensional binary sets. As expected, CC performs significantly better than the other baselines on account of being able to properly compress multi-modal classes, albeit requiring multiple passes. CC1 performs significantly worse than CC since one cluster is not able to appropriately compress multi-modal classes while maintaining the separation between the classes. LR and MLPC perform similarly to CC1. The proposed FBFC and FBFC* significantly outperform SBFC, highlighting the need for sparse high dimensional hashes to summarize multi-modal neighborhoods while avoiding overlap between per-class FBFs.

5.2.2 OpenML data

We consider classification (binary and multi-class) data sets from OpenML with numerical columns. We utilize two groups of data sets of following sizes: (i) 48 data sets with $d \in [10, 100]$, $n \le 50000$, and (ii) 10 data sets with $d \in [101, 1024]$, $n \le 10000$ (see precise details in Supplement S3.4). We consider the same procedure as above of tuning hyper-parameters for the 10-fold cross-validated accuracy for all baselines and the proposed scheme relative to the best k−NNC accuracy. The results, aggregated across all data sets in the two groups, are summarized in Figures 2c and 2d.

As with synthetic data, the results indicate that FBFC* is able to match the performance of k−NNC for both $d \in [10, 100]$ and $d \in [100, 1024]$ on a varied set of real data sets, with the binary FBFC falling behind

on the lower dimensional sets. `FBFC` has a median relative performance of 0.12 for $d \in [10, 100]$ compared to 0.05 for `FBFC`*, justifying the novel non-binary `FBF`. The binary `FBFC` matches k–NNC in higher dimensions – both `FBFC` and `FBFC`* have a median relative performance of around 0.01. CC performs best relative to k–NNC overall. Both the proposed schemes are fairly competitive with the multiple-pass CC baseline while significantly outperforming CC1 and SBFC. `FBFC` and `FBFC`* are competitive to LR and MLPC for the lower dimensional sets (relative performance of 0.07 and 0.06 for LR and MLPC respectively) while edging ahead in the higher dimensional sets (relative performance of 0.04 and 0.05 for LR and MLPC respectively).

5.2.3 Vision data

As a final comparison, we consider 4 popular vision data sets[2]. In this experiment, we only consider `FBFC`* (omitting `FBFC`) and tune hyper-parameters for all methods with a held-out set and report the accuracy of the best hyper-parameters on the pre-defined test set in Table 1. The results indicate that `FBFC`* is competitive to CC for Mnist, while outperforming all methods including k–NNC significantly on Cifar10 & Cifar100. With Fashion-Mnist, CC, LR and MLPC perform competitively to k–NNC while `FBFC`* falls significantly behind. `FBFC`* significantly outperforms CC1 and SBFC baselines as in the previous comparisons.

Table 1: Test accuracy (in %) for vision sets.

Method	Mnist	F-Mnist	Cifar10	Cifar100
k–NNC	97.36	85.90	31.65	14.38
CC1	82.23	70.34	24.72	7.63
CC	96.26	84.66	31.86	13.09
SBFC	13.60	26.10	11.27	1.88
LR	92.09	84.30	28.37	7.65
MLPC	96.06	84.27	28.96	7.09
FBFC*	95.69	80.02	36.73	16.34

5.3 Scaling

We evaluate the scaling of the parallelized `FBFC` training (Algorithm 1 (TrainFBFC)) with the number of parallel threads. For fixed hyper-parameters, we average runtimes (and speedups) over 10 repetitions for each of the 6 data sets (see Table S1 in Supplement S3) and present the results in Figure 3. The results indicate that the parallelized implementation of our proposed scheme scales very well for up to 8 threads for the larger data sets. The parallelism shows significant gains (up to $2\times$) even for the tiny Digits data set, demonstrating the parallelizability of the `FBFC` training.
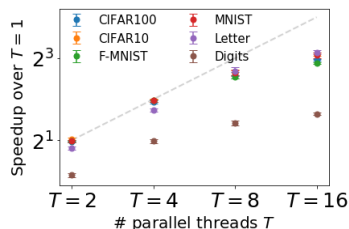

Figure 3: Scaling of parallelized `FBFC` training with T threads for $T = 1, 2, 4, 8, 16$. The gray line corresponds to linear scaling. *Please view in color.*

5.4 Problem insights through class similarities

We consider some of the vision data sets and explore the inter-class similarities for the problems. For each data set, we report the top 2 most similar class pairs based on their respective trained `FBFC` in Figure 4. For MNIST, the most similar pairs of digits are $(4, 9)$ and $(7, 9)$. This is somewhat validated by the images where these pairs are digits are visually hard to distinguish. In Fashion-MNIST, the hard pairs are (trouser, dress) and (pullover, coats). Trousers have the same long structure as dresses, and pullovers have the same structure of a top with two long arm sleeves. For CIFAR10, the most similar label pairs as per the `FBFC`

---

[2]See Table S1 in Supplement S3 for data details. Note that we are not claiming to be competitive with the state-of-the-art deep learning classifiers – we are merely demonstrating the capability of our proposed scheme to be competitive to k–NNC (and other single-pass baselines) on data sets from varied domains.
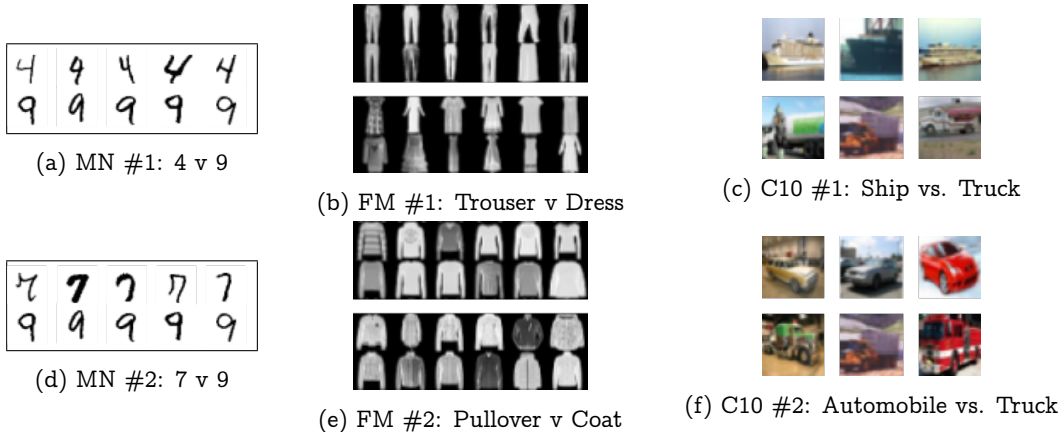
(a) MN #1: 4 v 9

(b) FM #1: Trouser v Dress

(c) C10 #1: Ship vs. Truck

(d) MN #2: 7 v 9

(e) FM #2: Pullover v Coat

(f) C10 #2: Automobile vs. Truck

Figure 4: Label pairs for MNIST (MN), Fashion-MNIST (FM) and CIFAR10 (C10) with highest `FBF` similarities.

class similarities are "ship" vs. "truck" and "automobile" vs. "truck". Both ship and truck images usually have pictures of containers; trucks and automobiles are images of vehicles with headlights, wheels and such. The class similarities generated by `FBFC` seem reasonable for these data sets, implying that we can use this scheme to estimate class similarities in other problems where the class labels are not interpretable and there are no inter-class hierarchies.

6 Conclusions and future work

In this paper we proposed a novel neurosciene inspired Fly Bloom Filter based classifier (`FBFC`) that can be trained in an *embarrassingly parallelized* fashion in a single pass of the training set – a point never needs to be revisited, and the whole training data does not need to be in memory. The inference requires an efficient `FlyHash` followed by a very sparse dot product. On the theoretical side, we established conditions under which `FBFC` agrees with the nearest-neighbor classifier. We empirically validated our proposed scheme with over 50 data sets of varied data dimensionality and demonstrated that the predictive performance of our proposed classifier is competitive the the k-nearest-neighbor classifier and other single-pass classifiers.

In the future we will pursue theoretical guarantees for `FBFC` and `FBFC`* for general data in $\mathbb{R}^d$ by exploring other data dependent assumptions such as doubling measure. Utilizing the sparse and randomized nature of `FBFC`, we will also investigate differential privacy preserving properties of `FBFC` as well as robustness of `FBFC` to benign and adversarial perturbations.

References

Sanjoy Dasgupta, Timothy C Sheehan, Charles F Stevens, and Saket Navlakha. A neural data structure for novelty detection. *Proceedings of the National Academy of Sciences*, 115(51):13093–13098, 2018.

Sanjoy Dasgupta, Charles F Stevens, and Saket Navlakha. A neural algorithm for a fundamental computing problem. *Science*, 358(6364):793–796, 2017.

Demis Hassabis, Dharshan Kumaran, Christopher Summerfield, and Matthew Botvinick. Neuroscience-inspired artificial intelligence. *Neuron*, 95(2):245–258, 2017.

Koray Kavukcuoglu, Pierre Sermanet, Y-Lan Boureau, Karol Gregor, Michaël Mathieu, and Yann L Cun. Learning convolutional feature hierarchies for visual recognition. In *Advances in neural information processing systems*, pages 1090–1098, 2010.

Alex Krizhevsky, Ilya Sutskever, and Geoffrey E Hinton. Imagenet classification with deep convolutional neural networks. In *Advances in neural information processing systems*, pages 1097–1105, 2012.

Geoffrey E Hinton, Nitish Srivastava, Alex Krizhevsky, Ilya Sutskever, and Ruslan R Salakhutdinov. Improving neural networks by preventing co-adaptation of feature detectors. *arXiv preprint arXiv:1207.0580*, 2012.

Hugo Larochelle and Geoffrey E Hinton. Learning to combine foveal glimpses with a third-order boltzmann machine. In *Advances in neural information processing systems*, pages 1243–1251, 2010.

Volodymyr Mnih, Nicolas Heess, Alex Graves, et al. Recurrent models of visual attention. In *Advances in neural information processing systems*, pages 2204–2212, 2014.

L. Zhou, L. Wang, X. Ge, and Q. Shi. A clustering-based knn improved algorithm clknn for text classification. In *International Asia Conference on Informatics in Control, Automation and Robotics*, pages 212–215, 2010.

Hamid Parvin, Moslem Mohamadi, Sajad Parvin, Zahra Rezaei, and Behrouz Minaei. Nearest cluster classifier. In Emilio Corchado, Václav Snášel, Ajith Abraham, Michał Woźniak, Manuel Graña, and Sung-Bae Cho, editors, *Hybrid Artificial Intelligent Systems*, pages 267–275, Berlin, Heidelberg, 2012. Springer Berlin Heidelberg.

S. Oigiaroglou and G. Evangelidis. Efficient k-nn classification based on homogeneous clusters. *Artificial Intelligence Review*, 42:491–513, 2013.

S. Oigiaroglou and G. Evangelidis. RHC: A non-parametric cluster-based data reduction for efficient k-nn classification. *Pattern Analysis and Applications*, 19:93–109, 2016.

A-J. Gallego, J. Calvo-Zaragoza, J. J. Valero-Mas, and J. R. Rico-Juan. Clustering-based k-nearest neighbor classification for large-scale data with neural codes representation. *Pattern Recognition*, 74:531–543, 2018.

J. Gou, W. Qiu, Z. Yi, Y. Xu, Q. Mao, and Y. Zhan. A local mean representation-based k-nearest neighbor classifier. *ACM Transactions on Intelligent Systems and Technology*, 10(3):1–25, 2019.

S. M. Omohundro. Five balltree construction algorithms. Technical report, International Computer Science Institute, Berkeley, CA, 1989.

A. Beygelzimer, S. Kakade, and J. Langford. Cover tree for nearest neighbor. In *International Conference on Machine Learning*, pages 97–104, 2006.

S. Dasgupta and K. Sinha. Randomized partition trees for nearest neighor search. *Algorithmica*, 72(1):237–267, 2015.

Parikshit Ram and Kaushik Sinha. Revisiting kd-tree for nearest neighbor search. In *Proceedings of the 25th ACM SIGKDD International Conference on Knowledge Discovery and Data Mining*, pages 1378–1388, 2019.

A. Gionis, P. Indyk, and R. Motwani. Similarity search in high dimensions via hashing. In *International Conference on Very large Data Bases*, pages 518–529, 1999.

A. Andoni and P. Indyk. Near-optimal hashing algorithms for approximate nearest neighbor in high dimensions. *Communications of the ACM*, 52(1):117–122, 2008.

A. Kirsch and M. Mitzenmacher. Distance sensitive bloom filters. In *Meeting in Algorithm Engineering & Experiments*, pages 41–50, 2006.

Y. Hua, B. Veeravalli, and D. Feng. Locality-sensitive bloom filter for approximate membership query. *IEEE Trans. Comput.*, 61(6):817–830, 2012.

S. Vempala. *The Random Projection Method*, volume 65 of *DIMACS Series in Discrete Mathematics and Theoretical Computer Science*. DIMACS/AMS, 2004.

Parikshit Ram and Alexander G Gray. Maximum inner-product search using cone trees. In *Proceedings of the 18th ACM SIGKDD International Conference on Knowledge Discovery and Data Mining*, pages 931–939, 2012.

Anshumali Shrivastava and Ping Li. Asymmetric lsh (alsh) for sublinear time maximum inner product search (mips). In *Advances in Neural Information Processing Systems*, pages 2321–2329, 2014.

A. B. Tsybakov. Optimal aggregation of classifiers in statistical learning. *The Annals of Statistics*, 32(1): 135–166, 2004.

J. Y. Audibert and A. B. Tsybakov. Fast learning rates for plug-in classifiers. *The Annals of Statistics*, 35(2):608–633, 2007.

Jan N Van Rijn, Bernd Bischl, Luis Torgo, Bo Gao, Venkatesh Umaashankar, Simon Fischer, Patrick Winter, Bernd Wiswedel, Michael R Berthold, and Joaquin Vanschoren. Openml: A collaborative science platform. In *Joint european conference on machine learning and knowledge discovery in databases*, pages 645–649. Springer, 2013.

Moses S Charikar. Similarity estimation techniques from rounding algorithms. In *Proceedings of the thiry-fourth annual ACM symposium on Theory of computing*, pages 380–388, 2002.

Diederik P Kingma and Jimmy Ba. Adam: A method for stochastic optimization. *arXiv preprint arXiv:1412.6980*, 2014.

Fabian Pedregosa, Gaël Varoquaux, Alexandre Gramfort, Vincent Michel, Bertrand Thirion, Olivier Grisel, Mathieu Blondel, Peter Prettenhofer, Ron Weiss, Vincent Dubourg, et al. Scikit-learn: Machine learning in python. *Journal of machine learning research*, 12(Oct):2825–2830, 2011.

Isabelle Guyon. Design of experiments of the nips 2003 variable selection benchmark. In *NIPS 2003 workshop on feature extraction and feature selection*, 2003.

Rong-En Fan, Kai-Wei Chang, Cho-Jui Hsieh, Xiang-Rui Wang, and Chih-Jen Lin. Liblinear: A library for large linear classification. *Journal of machine learning research*, 9(Aug):1871–1874, 2008.

Mark Schmidt, Nicolas Le Roux, and Francis Bach. Minimizing finite sums with the stochastic average gradient. *Mathematical Programming*, 162(1-2):83–112, 2017.

Aaron Defazio, Francis Bach, and Simon Lacoste-Julien. Saga: A fast incremental gradient method with support for non-strongly convex composite objectives. In *Advances in neural information processing systems*, pages 1646–1654, 2014.

S1 Discussion on non-binary FBFC

Note that the jth coordinate of any FBF* w_i diminishes as the number of training examples x' with label i and nonzero j^{th} coordinate in their FlyHash $h(x')$ increases. In fact, we can control the number of data points that can affect the value of w_{ij}. To see this, choose any small $\epsilon > 0$ such that if $w_{ij} \leq \epsilon$, then we

can effectively assume $w_{ij} \approx 0$. Suppose $t = |\{(x', y') \in S : y' = i \text{ and } (h(x'))_j = 1\}|$. Then it is easy to see that,

$$w_{ij} = (1-c)^t \leq e^{-ct} \leq \epsilon \Rightarrow t \geq \frac{1}{c}\ln(1/\epsilon)$$

That means even if the set $|\{(x', y') \in S : y' = i \text{ and } (h(x'))_j = 1\}|$ may contain $t' > t$ data points, only t of them control the value of w_{ij}. More importantly, (i) t can be controlled by choosing appropriate c, and (ii) using the similarity preservation of the projection matrix M^s_m, any test point x with $(h(x))_j = 1$ will be close to those t data point with high probability.

S2   Supplementary material from Section 4

Stating `FlyHash` definition for completeness:

The basic building block of our proposed algorithm is a fruit-fly olfactory circuit inspired `FlyHash` function, first introduced by Dasgupta et al. [2017]. For $x \in \mathbb{R}^d$, the `FlyHash` function $h: \mathbb{R}^d \to \{0,1\}^m$ is defined as,

$$h(x) = \Gamma_\rho(M^s_m x), \tag{S1}$$

where $M^s_m \in \{0,1\}^{m \times d}$ is the randomized sparse lifting binary matrix with $s \ll d$ nonzero entries in each row, and $\Gamma_\rho: \mathbb{R}^m \to \{0,1\}^m$ is the winner-take-all function converting a vector in $\mathbb{R}^m$ to one in $\{0,1\}^m$ by setting the highest ρ elements to 1 and the rest to zero. For ease of notation, we use M instead of M^s_m.

S2.1   Proof of Lemma 1

Stating Lemma 1 for completeness:

Lemma S1. *Fix any $x \in \mathbb{R}^d$ and let $h(x) \in \{0,1\}^m$ be its FlyHash using equation S1. Let $x^i_{NN} = \operatorname{argmin}_{(x',y') \in S^i} \|x - x'\|$ for $i \in \{0, 1\}$, where $\|\cdot\|$ is any distance metric. Let $A_{S^1} = \{\theta : \cap_{(x',y') \in S^1} \theta^\top x' < \tau_{x'}(\rho/m)\}$ and $A_{S^0} = \{\theta : \cap_{(x',y') \in S^0} \theta^\top x' < \tau_{x'}(\rho/m)\}$. Then the following holds, where the expectation is taken over the random choice of projection matrix M.*

(i) $\mathbb{E}_M(\frac{w_1^\top h(x)}{\rho}) = \Pr_{\theta \sim Q}\left(A_{S^1} \mid \theta^\top x \geq \tau_x(\rho/m)\right)$

(ii) $\mathbb{E}_M(\frac{w_0^\top h(x)}{\rho}) = \Pr_{\theta \sim Q}\left(A_{S^0} \mid \theta^\top x \geq \tau_x(\rho/m)\right)$

(iii) $\mathbb{E}_M(\frac{w_1^\top h(x)}{\rho}) \geq 1 - \sum_{x' \in S^1} q(x, x')$

(iv) $\mathbb{E}_M(\frac{w_1^\top h(x)}{\rho}) \leq 1 - q(x, x^1_{NN})$

(v) $\mathbb{E}_M(\frac{w_0^\top h(x)}{\rho}) \geq 1 - \sum_{x' \in S^0} q(x, x')$

(vi) $\mathbb{E}_M(\frac{w_0^\top h(x)}{\rho}) \leq 1 - q(x, x^0_{NN})$

Proof. Part (i) and (ii) follows from simple application of Lemma 2 of Dasgupta et al. [2018] to class specific `FBF`s. Part (iii) and (v) follows from simple application of Lemma 3 of Dasgupta et al. [2018] to class specific `FBF`s. For part (iv), simple application of Lemma 3 of Dasgupta et al. [2018] to `FBF` w_1 ensures that for any $x' \in S^1, \mathbb{E}_M(\frac{w_1^\top h(x)}{\rho}) \leq 1 - q(x, x')$. Clearly, $\mathbb{E}_M(\frac{w_1^\top h(x)}{\rho}) \leq 1 - q(x, x^1_{NN})$. Applying similar argument, part (vi) also holds. □

S2.2   Proof of Theorem 3

We analyze classification performance of `FBFC` trained on a training set $S = \{(x_i, y_i)\}_{i=1}^{n_0+n_1} \subset \mathcal{X} \times \{0,1\}$, where $S = S^1 \cup S^0$, $S^0 \subset S$ with label 0 and $S^1 \subset S$ with label 1, satisfying $|S^0| = n_0$ and $|S^1| = n_1$ and $n = \max\{n_0, n_1\}$. For appropriate choice of m, let $w_0, w_1 \in \{0,1\}^m$ be the `FBF`s constructed using S^0 and S_1 respectively. In Theorem 3, we consider a special case where examples from each class have binary feature vectors with fixed number of ones. In particular, $\mathcal{X} = \mathcal{X}_b = \{x \in \{0,1\}^d : |x|_1 = b < d\}$.

Restating Theorem 3 for completeness:

Theorem S2. *Let S be a training set as given above. Fix any $\delta \in (0,1)$, and set $\rho \geq \frac{12}{\mu}\ln(4/\delta)$, $m \geq (d/b)n\rho$, and $s = \log_{d/b}(m/\rho)$, where $\mu = \min\left\{\mathbb{E}_M\left(\frac{w_0^\top h(x)}{\rho}\right), \mathbb{E}_M\left(\frac{w_1^\top h(x)}{\rho}\right)\right\}$ and $h(x)$ is the FlyHash function from equation S1. For any test example $x \in \mathcal{X}$, let its closest point from S measured using ℓ_1 metric be x_{NN}, having label $y_{NN} \in \{0,1\}$, satisfies, (i) $\|x - x_{NN}\|_1 \leq \frac{2b(1-b/d)}{3s}$, and (ii) $\|x - x_i\|_1 \geq 2b(1-b/d)$ for all $(x_i, y_i) \in S$, with $y_i \neq y_{NN}$. Let $w_0, w_1 \in \{0,1\}^m$ be the FBFs constructed using S^0 and S^1 respectively. Then, with probability at least $1-\delta$ (over the random choice of projection matrix M), prediction of FBFC on x agrees with the prediction of 1-NN classifier on x.*

Proof. We first show that a result similar to the one we wish to prove holds in expectation (for exact statement, please see Lemma S3 below). Using this result and standard concentration results presented in lemma S4, we show that the desired result holds with high probability, provided ρ is large.

Using Lemma S3, we show that $\mathbb{E}_M\left(\frac{w_1^\top h(x)}{\rho}\right) \leq s\epsilon$ and $\mathbb{E}_M\left(\frac{w_0^\top h(x)}{\rho}\right) \geq 1 - \frac{b}{d}$. Therefore, if ϵ is restricted in the range $\left(0, \frac{(1-b/d)}{(\log_{d/b}(m/\rho))}\right)$, then $\mathbb{E}_M\left(\frac{w_1^\top h(x)}{\rho}\right) < \mathbb{E}_M\left(\frac{w_0^\top h(x)}{\rho}\right)$ which ensures that prediction of FBFC on x agrees with prediction of 1-NN classifier on x in expectation. Now, using Lemma S4, with probability at least $1-\delta$, we have, $\frac{w_1^\top h(x)}{\rho} \leq \frac{3}{2}\mathbb{E}_M\left(\frac{w_1^\top h(x)}{\rho}\right) \leq \frac{3s\epsilon}{2}$ and $\frac{w_0^\top h(x)}{\rho} \geq \frac{1}{2}\mathbb{E}_M\left(\frac{w_0^\top h(x)}{\rho}\right) \geq \frac{1}{2}\left(1 - \frac{b}{d}\right)$. Restricting ϵ in the range $\left(0, \frac{(1-b/d)}{3\log_{d/b}(m/\rho)}\right)$, ensures that $\|x - x_{NN}\|_1 = 2b\epsilon \leq \frac{2(1-b/d)}{3\log_{d/b}(m/\rho)}$, and with probability at least $1-\delta$, $\frac{w_0^\top h(x)}{\rho} < \frac{w_1^\top h(x)}{\rho}$. The result follows. $\qquad\square$

Lemma S3. *Let S be a training set as given above. For any test example $x \in \mathcal{X}$, let its closest point from S measured using ℓ_1 metric be x_{NN} having label $y_{NN} \in \{0,1\}$. Assume that for all $(x_i, y_i) \in S$, with $y_i \neq y_{NN}$, $\|x - x_i\|_1 \geq 2b(1-b/d)$ and x_{NN} satisfies $\|x - x_{NN}\|_1 \leq \frac{2b(1-b)}{\log_{d/b}(m/\rho)}$, where $m \geq (d/b)n\rho$. Let $s = \log_{d/b}(m/\rho)$ and $w_0, w_1 \in \{0,1\}^m$ be the FBFs constructed using S^0 and S^1 respectively. Then, in expectation (over the random choice of projection matrix M), prediction of FBFC on x agrees with the prediction of 1-NN classifier on x.*

Proof. Without loss of generality, assume assume that x_{NN} satisfies the relation $\|x - x_{NN}\|_1 = 2b\epsilon$ for some $0 < \epsilon < 1$ and $y_{NN} = 1$. Clearly, 1-NN classifier will predict x's class label to be 1.

Let $h(x) \in \{0,1\}^m$ be the FlyHash function from equation S1. To ensure that prediction of FBFC on x agrees with that of 1-NN classifier on expectation, we need to show that $\mathbb{E}_M\left(\frac{w_1^\top h(x)}{\rho}\right) < \mathbb{E}_M\left(\frac{w_0^\top h(x)}{\rho}\right)$. Our plan is to show that upper bound of $\mathbb{E}_M\left(\frac{w_1^\top h(x)}{\rho}\right)$ is strictly smaller then lower bound of $\mathbb{E}_M\left(\frac{w_0^\top h(x)}{\rho}\right)$. Towards this end, for any $x \in \mathcal{X}_b$, set the threshold $\tau_x(k/m)$ to be s, whose value will be chosen later. Then we have,

$$
\begin{aligned}
\Pr_{\theta \sim Q}(\theta \cdot x \geq \tau_x(\rho/m)) &= \Pr_{\theta \sim Q}(\theta \cdot x \geq s) \\
&= \Pr_{\theta \sim Q}(\theta \cdot x = s) \\
&= \frac{\binom{b}{s}}{\binom{d}{s}} \approx \left(\frac{b}{d}\right)^s
\end{aligned}
$$

where the second inequality follows from the fact that θ has exactly s ones and maximum value of $\theta^\top x$ is s. Since $\Pr_{\theta \sim Q)}(\theta^\top x \geq \tau_x(\rho/m)) = \rho/m$, we have $s \approx \frac{\log(m/\rho)}{\log(d/b)} = \log_{d/b}(m/\rho)$. Additionally, from Lemma 6 of Dasgupta et al. [2018] we have ,

$$
q(x, x') \approx \left(\frac{x^\top x'}{b}\right)^s \tag{S2}
$$

This approximation is excellent when c is small relative to $x \cdot x'$. We will henceforth take it to be equality. It is easy to check that for any $x, x' \in \mathcal{X}_b$, $\|x - x'\|_1 = 2(b - x \cdot x')$. Therefore, $\|x - x_{NN}\| = 2b\epsilon$ implies $x^\top x_{NN} = b(1-\epsilon)$ and for all $(x', y') \in S^0$, $\|x - x'\|_1 \geq 2b(1 - b/d)$ implies $x^\top x' \leq (b/d)b$. Therefore, using equation S2, we have $q(x, x_{NN}) = \left(\frac{x^\top x_{NN}}{b}\right)^s = (1 - \epsilon)^s \geq 1 - s\epsilon$. Combining this with

14

part (iv) of Lemma S1, we have $\mathbb{E}_M \left(\frac{w_1^\top h(x)}{\rho} \right) \leq 1 - q(x, x_{NN}) \leq 1 - (1 - s\epsilon) = s\epsilon$. Since for each $(x', y') \in S^0$, $x^\top x' \leq (b/d)b$, we have $q(x, x') = \left(\frac{x \cdot x'}{b} \right)^s \leq \left(\frac{b}{d} \right)^s = \rho/m$. Combining this with part (v) of Lemma S1, we have $\mathbb{E}_M \left(\frac{w_0^\top h(x)}{\rho} \right) \geq 1 - \sum_{(x', y') \in S^0} q(x, x') \geq 1 - \frac{n_0 \rho}{m} \geq 1 - b/d$. To ensure that the lower bound of $\mathbb{E}_M \left(\frac{w_0^\top h(x)}{\rho} \right)$ is strictly larger than upper bound of $\mathbb{E}_M \left(\frac{w_1^\top h(x)}{\rho} \right)$, we need, $s\epsilon < (1 - b/d) \Rightarrow \epsilon < \frac{(1-b/d)}{s} = \frac{(1-b/d)}{\log_{d/b}(m/\rho)}$, which ensures $\|x - x_{NN}\|_1 = 2b\epsilon \leq \frac{2b(1-b/d)}{\log_{d/b}(m/\rho)}$.

Since for any test data point x, its closet point in S can also have label 0, we simply replace n_0 by $n = \max\{n_0, n_1\}$. $\square$

S2.3   Auxiliary Lemma and its proof

The following concentration result is standard and a similar form has appeared in Dasgupta et al. [2018].

Lemma S4. *Let* $x_1, \ldots, x_{n_1} \in \mathcal{X}_b$ *be the unlabeled examples of* S^1 *and let* $\tilde{x}_1, \ldots, \tilde{x}_{n_0} \in \mathcal{X}_b$ *be the unlabeled examples of* S^0 *from Lemma S3. Pick any* $\delta \in (0, 1)$ *and* $x \in \mathcal{X}_b$. *With probability at least* $1 - \delta$ *over the choice of random projection matrix* M, *the following holds,*
(i) $\frac{1}{2}\mathbb{E}_M \left(\frac{w_1^\top h(x)}{\rho} \right) \leq \frac{w_1^\top h(x)}{\rho} \leq \frac{3}{2}\mathbb{E}_M \left(\frac{w_1^\top h(x)}{\rho} \right)$
(ii) $\frac{1}{2}\mathbb{E}_M \left(\frac{w_0^\top h(x)}{\rho} \right) \leq \frac{w_0^\top h(x)}{\rho} \leq \frac{3}{2}\mathbb{E}_M \left(\frac{w_0^\top h(x)}{\rho} \right)$
provided $\rho \cdot \min \left\{ \mathbb{E}_M \left(\frac{w_0^\top h(x)}{\rho} \right), \mathbb{E}_M \left(\frac{w_1^\top h(x)}{\rho} \right) \right\} \geq 12\ln(4/\delta)$.

Proof. We will only prove part (i) since part (ii) is similar. Let $h(x), h(x_1), \ldots, h(x_{n_1})$ be the projected-and-thresholded versions of $x, x_1, \ldots, x_{n_1}$ respectively. Define random variables $U_1, \ldots, U_m \in \{0, 1\}$ as follows:

$$U_j = \begin{cases} 1, & \text{if } h(x_1)_j = \cdots = h(x_{n_1})_j = 0 \text{ and } h(x)_j = 1 \\ 0, & \text{otherwise} \end{cases}$$

The U_j are i.i.d. and

$$\mathbb{E}_M(U_j) = \Pr_M(h(x)_j = 1) \times$$
$$\Pr_M \left(h(x_1)_j = \cdots = h(x_{n_1})_j = 0 \mid h(x)_j = 1 \right)$$
$$= \frac{\rho}{m} \mathbb{E}_M \left(\frac{w_1^\top h(x)}{\rho} \right)$$

where we have used the fact that $\Pr_M(h(x)_j = 1) = \Pr_{\theta \sim Q}(\theta^\top x \geq \tau_x(\rho/m)) = \rho/m$ and using Lemma 2 of the supplementary material of Dasgupta et al. [2018], $\Pr_M \left(h(x_1)_j = \cdots = h(x_{n_1})_j = 0 \mid h(x)_j = 1 \right) = \mathbb{E}_M \left(\frac{w_1^\top h(x)}{\rho} \right)$. Therefore, $\mathbb{E}_M(U_1 + \cdots + U_m) = \rho \cdot \mathbb{E}_M \left(\frac{w_1^\top h(x)}{\rho} \right)$. Let $\mu_1 = \mathbb{E}_M \left(\frac{w_1^\top h(x)}{\rho} \right)$. By multiplicative Chernoff bound for any $0 < \epsilon < 1$, we have,

$$\Pr_M (U_1 + \cdots + U_m \geq (1 + \epsilon)\rho\mu_1) \leq \exp(-\epsilon^2 \rho\mu_1/3)$$

$$\Pr_M (U_1 + \cdots + U_m \leq (1 - \epsilon)\rho\mu_1) \leq \exp(-\epsilon^2 \rho\mu_1/2)$$

Setting $\epsilon = 1/2$ and bounding right hand side of each of the above two inequalities by $\delta/4$, ensures that part (i) holds with probability at least $1 - \frac{\delta}{2}$ provided $\rho \cdot \mathbb{E}_M \left(\frac{w_1^\top h(x)}{\rho} \right) \geq 12\ln(4/\delta)$. $\square$

S2.4   Result for multi-class classification

Theorem S2 can be easily extended to multi-class classification problem involving L classes in a straight forward manner by applying concentration result to each of the $\left(\frac{w_i^\top h(x)}{\rho} \right)$, for $i \in [L]$, and using a union bound.

Corollary S5. *Given a training set* $S = \{(x_i, y_i)\}_{i=1}^{\sum_{j=1}^{L-1} n_j} \subset \mathcal{X}_b \times \mathcal{Y} \subset \{0,1\}^d \times \{0,1,\ldots,L-1\}$ *of size* $\sum_{i=0}^{L-1} n_i$, *let* $S = \cup_{i=0}^{L-1} S^i$, *where* S^i *is the subset of* S *with label* i *satisfying* $|S^i| = n_i$ *and* $n = \max\{n_0, \ldots, n_{L-1}\}$. *For any test example* $x \in \mathcal{X}_b$, *let its closest point from* S *measured using* ℓ_1 *metric be* x_{NN} *having label* $y_{NN} \in \{0, \ldots, L-1\}$. *Fix any* $\delta \in (0,1)$ *and set* $\rho \geq \frac{12}{\mu} \ln(2L/\delta)$, $m \geq (d/b)n\rho$, *and* $s = \log_{d/b}(m/\rho)$, *where* $\mu = \min \left\{ \mathbb{E}_M \left(\frac{w_0^\top h(x)}{\rho} \right), \ldots, \mathbb{E}_M \left(\frac{w_{L-1}^\top h(x)}{\rho} \right) \right\}$ *and* $h(x)$ *is the* `FlyHash` *function from equation S1. Assume that for all* $(x_i, y_i) \in S$, *with* $y_i \neq y_{NN}$, $\|x - x_i\|_1 \geq 2b(1 - b/d)$ *and* x_{NN} *satisfies* $\|x - x_{NN}\|_1 \leq \frac{2b(1-b/d)}{3s}$. *Let* $w_0, \ldots, w_{L-1} \in \{0,1\}^m$ *be the* `FBFs` *constructed using* $S^0, \ldots, S^{L-1}$ *respectively. Then, with probability at least* $1 - \delta$ *(over the random choice of projection matrix* M*), prediction of* `FBFC` *on* x *agrees with the prediction of 1-NN classifier on* x.

S2.5 Proof of Theorem 4

We analyze classification performance of `FBFC` trained on a training set $S = \{(x_i, y_i)\}_{i=1}^{n_0 + n_1} \subset \mathcal{X} \times \{0,1\}$, where $S = S^1 \cup S^0$, $S^0 \subset S$ with label 0 and $S^1 \subset S$ with label 1, satisfying $|S^0| = n_0$ and $|S^1| = n_1$ and $n = \max\{n_0, n_1\}$. For appropriate choice of m, let $w_0, w_1 \in \{0,1\}^m$ be the `FBFs` constructed using S^0 and S_1 respectively. In Theorem 3, we consider a special case where we make permutation invariant distribution assumption. Permutation invariant distribution in the `FBF` context was first introduced in Dasgupta et al. [2018] and is defined as follows: a distribution P over $\mathbb{R}^d$ is permutation invariant if for any permutation σ of $\{1, 2, \ldots, d\}$ and any $x = (x_1, \ldots, x_d) \in \mathbb{R}^d$, $P(x_1, \ldots, x_d) = P(x_{\sigma(1)}, \ldots, x_{\sigma(d)})$. Restating Theorem 4 for completeness.

Theorem S6. *Let* S *be a training set as given above. Fix any* $\delta \in (0,1)$, $s \ll d$, *and set* $\rho \geq \frac{48}{\mu} \ln(8/\delta)$ *and* $m \geq 14n\rho/\delta$, *where* $\mu = \min \left\{ \mathbb{E}_M \left(\frac{w_0^\top h(x)}{\rho} \right), \mathbb{E}_M \left(\frac{w_1^\top h(x)}{\rho} \right) \right\}$, $h(x)$ *is the* `FlyHash` *function from equation S1, and* $w_0, w_1 \in \{0,1\}^m$ *are the* `FBFs` *constructed using* S^0 *and* S^1 *respectively. For any test example* $x \in \mathbb{R}^d$, *sampled from a permutation invariant distribution, let* x_{NN} *be its nearest neighbor from* S *measured using* ℓ_∞ *metric, which satisfies* $\|x - x_{NN}\|_\infty \leq \Delta/s$, *where* $\Delta = \frac{1}{2} (\tau_x(2\rho/m) - \tau_x(\rho/m))$ *and has label* $y_{NN} \in \{0,1\}$. *Then, with probability at least* $1 - \delta$ *(over the random choice of projection matrix* M*), prediction of* `FBFC` *on* x *agrees with the prediction of 1-NN classifier on* x.

Proof. Without loss of generality, assume that $y_{NN} = 1$. For the case when $y_{NN} = 0$, is similar. Prediction of `FBFC` on x agrees with the prediction of 1-NN classifier whenever $(w_1^\top h(x)/\rho) < (w_0^\top h(x)/\rho)$. We first show that $\mathbb{E}_M (w_1^\top h(x)/\rho) < \mathbb{E}_M (w_0^\top h(x)/\rho)$ with high probability and then using standard concentration bound presented in lemma S4, we achieve the desired result. Since $\|x - x_{NN}\|_\infty \leq \Delta/s$, using lemma 9 of Dasgupta et al. [2018], we get $q(x, x_{NN}) \geq 1/2$. Combining this with part (iv) of lemma S1, we get $\mathbb{E}_M (w_1^\top h(x)/\rho) \leq 1/2$. Next, since x is sampled from a permutation invariant distribution, using corollary 11 of Dasgupta et al. [2018], we get $\mathbb{E}_x q(x, x_i) = \rho/m$ for each $x' \in S^0$, and thus using linearity of expectation, $\mathbb{E}_x \left(\sum_{x' \in S^0} q(x, x') \right) = \sum_{x' \in S^0} \mathbb{E}_x q(x, x') = \rho n_0/m$. For any $\alpha > 0$, using Markov's inequality,

$$\Pr \left(\sum_{x' \in S^0} q(x, x') > \alpha \right) \leq \frac{\mathbb{E}_x \left(\sum_{x' \in S^0} q(x, x') \right)}{\alpha} = \frac{\rho n_0}{m\alpha} \leq \frac{\delta}{2}.$$

Therefore, $\sum_{x' \in S^0} q(x, x') \leq \alpha$ with probability at least $1 - \delta/2$ for $m \geq \frac{2\rho n_0}{\alpha\delta}$. Combining this with part (v) of lemma S1, we immediately get, $\mathbb{E}_M (w_0^\top h(x)/\rho) \geq 1 - \alpha$ with probability at least $1 - \delta/2$. It is easy to see that for $\alpha < 1/2$, $\mathbb{E}_M (w_1^\top h(x)/\rho) < \mathbb{E}_M (w_0^\top h(x)/\rho)$ with probability at least $1 - \delta/2$, and thus in expectation, prediction of `FBFC` on x agrees with the prediction of 1-NN classifier on x. Using concentration bound and a smaller α, we next show that $(w_1^\top h(x)/\rho) < (w_0^\top h(x)/\rho)$ with probability at least $1 - \delta$. In particular, using $\epsilon = 1/4$ and $\delta = \delta/2$ in lemma S4, we see that with probability at least $1 - \delta/2$ the following holds: (i) $\frac{3}{4} \mathbb{E}_M (w_1^\top h(x)/\rho) \leq w_1^\top h(x)/\rho \leq \frac{5}{4} \mathbb{E}_M (w_1^\top h(x)/\rho)$, and (ii) $\frac{3}{4} \mathbb{E}_M (w_0^\top h(x)/\rho) \leq w_0^\top h(x)/\rho \leq \frac{5}{4} \mathbb{E}_M (w_0^\top h(x)/\rho)$ provided $\rho \cdot \min \left\{ \mathbb{E}_M (w_0^\top h(x)/\rho), \mathbb{E}_M (w_1^\top h(x)/\rho) \right\} \geq 48 \ln(8/\delta)$. Combining this with

the bounds on the expected values of the novelty scores, it is easy to see that with probability $1 - \delta$, $w_1^\top h(x)/\rho < w_0^\top h(x)/\rho$ whenever, $\frac{1}{2} \cdot \frac{5}{4} < (1 - \alpha) \cdot \frac{3}{4} \Rightarrow \alpha < 1/6$. Since $n = \max\{n_0, n_1\} \geq n_0$, setting $\alpha = 1/7$, which in turn requires $m \geq 14 n \rho/\delta$, the result follows. $\qquad\square$

The above result can be extended to multi-class classification problem in a straight forward manner.

S3 Supplementary material from Section 5

Implementation & Compute Resource:. The proposed novel classification scheme is implemented in Python 3.6 to fit the `scikit-learn` API [Pedregosa et al., 2011], but the current implementation is not optimized for computational performance. We use the `scikit-learn` implementation of various baselines we consider in our evaluations. To generate synthetic data sets, we use the `data.make_classification` functionality in `scikit-learn` [Guyon, 2003]. The experiments are performed on a 16-core 128GB machine running Ubuntu 18.04.

Table S1: Details of a subset of the data sets. For CIFAR-10 and CIFAR-100, we collapse the 3 color channels and then flatten the 32×32 images to points in $\mathbb{R}^{1024}$. For MNIST and Fashion-MNIST, we flatten the 28×28 images to points in $\mathbb{R}^{784}$.

DATA SET	n	d	L	EXPERIMENT
DIGITS	1797	64	10	OPENML
LETTERS	20000	16	26	OPENML
SEGMENT	2310	19	7	OPENML
GINA PRIOR 2	3468	784	10	OPENML
USPS	9294	256	10	OPENML
MADELINE	3140	259	2	OPENML
MNIST	60000	784	10	VISION
FASHION-MNIST	60000	784	10	VISION
CIFAR-10	50000	1024	10	VISION
CIFAR-100	50000	1024	100	VISION

S3.1 Dependence on `FBFC` hyper-parameters

We study the effect of the different hyper-parameters of FBFC– (i) the dimensionality of the `FlyHash` m, (ii) the per-row density s of the sparse binary projection matrix M_m^s, (iii) the NNZ ρ in the `FlyHash` after the winner-take-all operation, and (iv) the decay rate c of the FBF. For this analysis, we consider 6 data sets from OpenML – Digits, Letters, Segment, Gina Prior 2, USPS and Madeline (see Table S1 for data sizes). For every hyper-parameter setting, we compute the 10-fold cross-validated accuracy. We vary each hyper-parameter while fixing the others. The results for each of the hyper-parameters and data sets are presented in Figure S1 & S2. We evaluate the following configurations for the evaluation of each of the hyper-parameters:

▶ **`FlyHash` dimension** m: We try 10 values for $m \in [4d, 4096d]$ with $(s/d) \in \{0.1, 0.3\}$, $\rho \in \{8, 32\}$, $c \in \{0.5, 1\}$.
▶ **Projection density** s/d: We try 10 values for $(s/d) \in [0.1, 0.8]$ with $m \in \{256, 1024\}$, $\rho \in \{8, 32\}$, $c \in \{0.5, 1\}$.
▶ **`FlyHash` NNZ** ρ: We try 10 values for $\rho \in [4, 256]$ with $m \in \{256, 1024\}$, $(s/d) \in \{0.1, 0.3\}$, $c \in \{0.5, 1\}$.
▶ **FBF decay rate** c: We try 10 values for $c \in [0.2, 0.9]$ and $c = 1$ with $m \in \{256, 1024\}$, $(s/d) \in \{0.1, 0.3\}$, $\rho \in \{8, 32\}$.
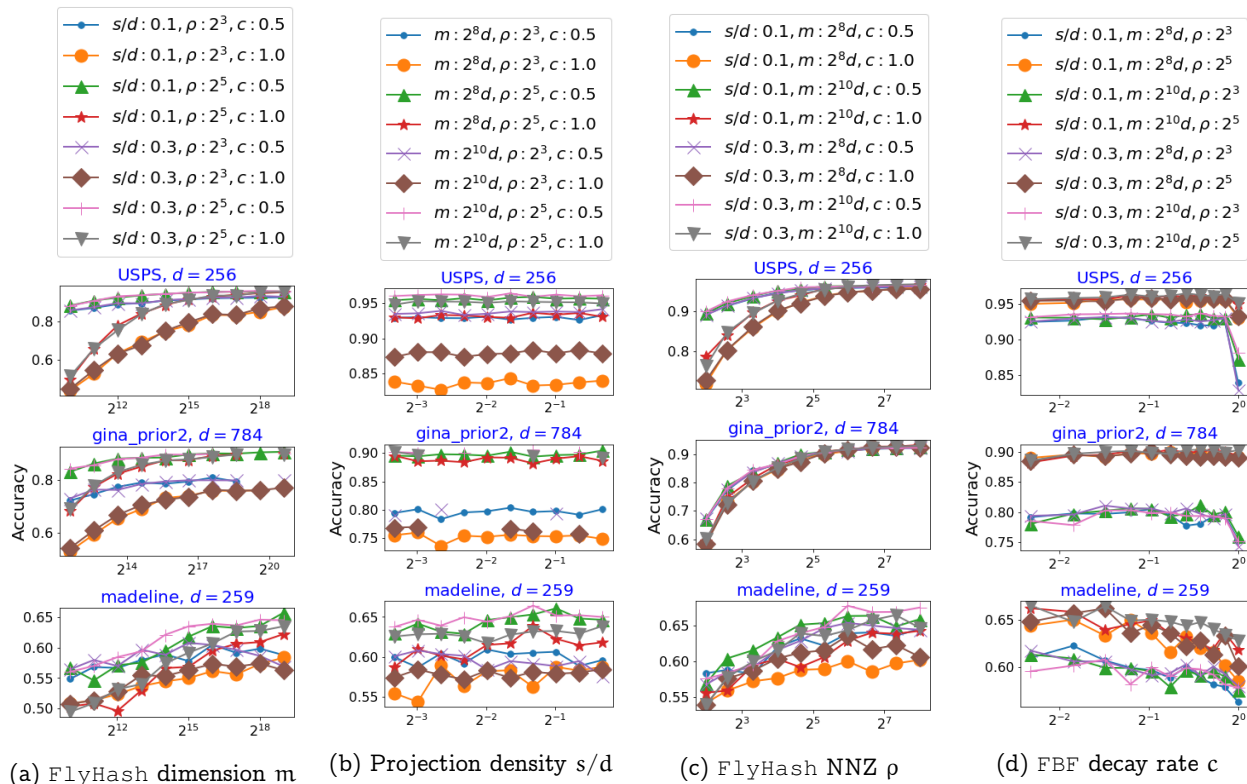
Figure S1: **FBFC hyper-parameter dependence – Part I.** Effect of the different FBFC hyper-parameters m, s, ρ, c on FBFC predictive performance for 3 data sets – the horizontal axes correspond to the hyper-parameter being varied while fixing the remaining hyper-parameters. The vertical axes correspond to the 10-fold cross-validated accuracy for the given hyper-parameter configuration (*higher is better*). Note the log scale on the horizontal axes. For the hyper-parameter c, c = 1 corresponds to the binary FBFC. *Please view in color.*

The results in Figures S1a & S2a indicate that, for fixed ρ increasing m improves the FBFC accuracy, aligning with the theoretical guarantees, up until an upper bound. This behavior is clear for high dimensional data sets. This behavior is a bit more erratic for the lower dimensional sets. Larger values of m improve performance, since it allows us to capture each class' distribution with smaller random overlap between each class' FBFs. But the theoretical guarantees also indicate that ρ needs to be large enough, and if m grows too large for any given k, the FBFC accuracy might not improve any further.

Figures S1b & S2b indicate that for lower dimensional data (such as d ≤ 20), increasing the projection density s improves performance up to a point (around s = 0.5), after which the performance starts degrading. This is probably because for smaller values of s, not enough information is captured by the sparse projection for small d; for large values of s, each row in the projection matrix M_m^s become similar to each other, hurting the similarity-preserving property of FlyHash. For higher dimensional data sets, the FBFC performance appears to be somewhat agnostic to s for any fixed m, ρ and c.

Figures S1c & S2c indicate that increase in ρ leads to improvement in FBFC performance since large values of ρ better preserve pairwise similarities. However, if ρ is too large relative to m, the sparsity of the subsequent per-class FBF go down, thereby leading to more overlap in the per-class FBFs. So ρ needs to large as per the theoretical analysis, but not too large.

Figures S1d & S2d indicate that the FBFC is somewhat agnostic to the FBF decay rate c for any value strictly less that 1 (corresponding to the binary FBF). But there is a significant drop in the FBFC performance from c < 1 to c = 1 across all data set – this behavior is fairly consistent and apparent.
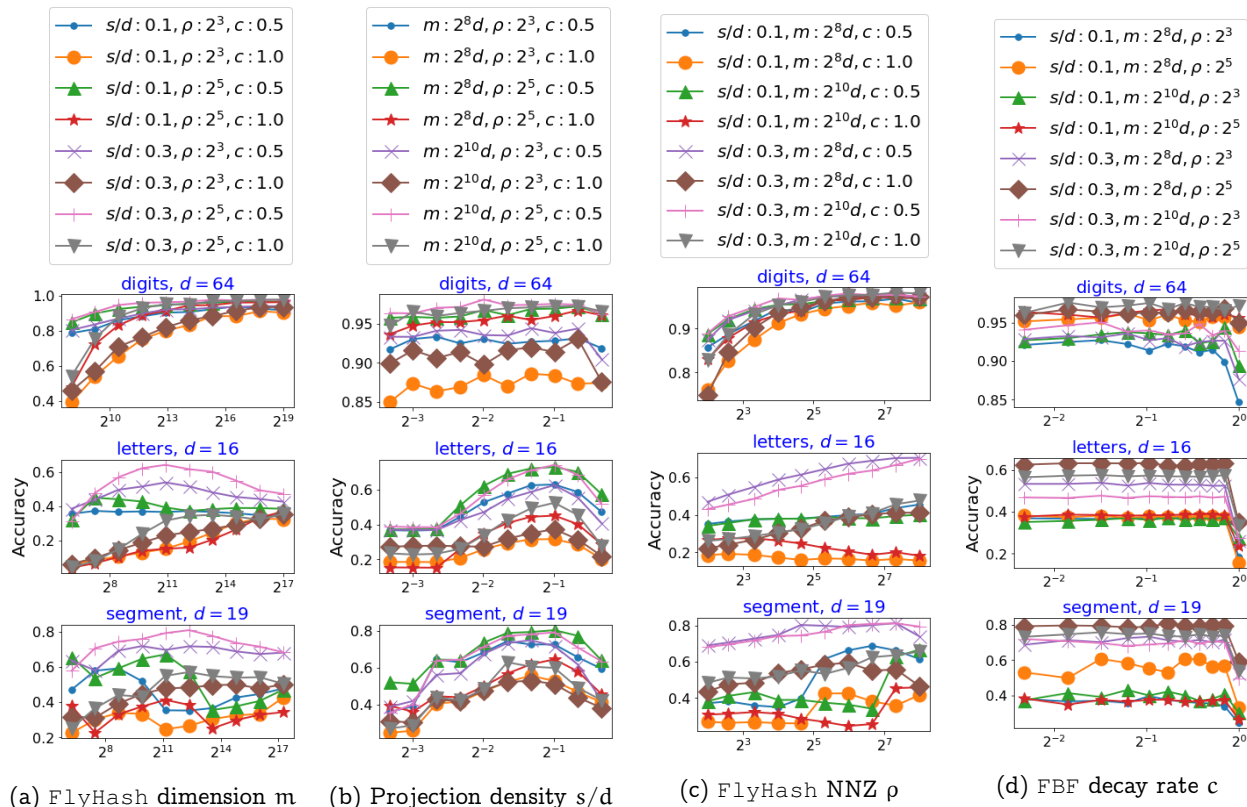
Figure S2: **FBFC hyper-parameter dependence – Part II.** Effect of the different FBFC hyper-parameters m, s, ρ, c on FBFC predictive performance for 3 data sets – the horizontal axes correspond to the hyper-parameter being varied while fixing the remaining hyper-parameters. The vertical axes correspond to the 10-fold cross-validated accuracy for the given hyper-parameter configuration (*higher is better*). Note the log scale on the horizontal axes. For the hyper-parameter c, $c = 1$ corresponds to the binary FBFC. *Please view in color.*

S3.2   Details on baselines

Here we detail all the baselines considered in our empirical evaluations and their respective hyper-parameter and the subsequent hyper-parameter optimization.

1. k**–NNC.** We consider the k–NNC as the primary baseline to match where we tune over the size of the neighborhood in the range $[1, 64]$ to maximize the 10-fold cross-validated accuracy for each data set (synthetic or real).

2. **CC1.** Classification based on a single prototype per class, where the prototype of a class is the geometric center of the class, which can be computed with a single pass of the data.

3. **SBFC.** Classification via a variation of FBFC where we utilize SimHash/SRP [Charikar, 2002] instead of FlyHash to give us the SimHash Bloom Filter classifier (SBFC). We consider this baseline to demonstrate the need of the highly sparse hashes generated by FlyHash– the hashes from SimHash are not explicitly designed to be sparse. The dimensionality of the SimHash m is the hyper-parameter we search over – we consider both projecting down in the range $m \in [1, d]$ (the traditional use) and projecting up $m \in [d, 2048d]$, where d is the data dimensionality. Note that for the same projected dimension m, SimHash is more expensive that FlyHash since SimHash involves a dense matrix-vector multiplication instead of the sparse matrix-vector in FlyHash.

4. **LR.** We consider logistic regression trained for a single epoch with a stochastic algorithm. We utilize the `scikit-learn` implementation (`linear_model.LogisticRegression`) and tune over the following hyper-parameters – (a) penalty type (ℓ_1/ℓ_2), (b) regularization $\in \left[2^{-10}, 2^{10}\right]$, (c) choice of solver (liblinear [Fan et al., 2008]/SAG [Schmidt et al., 2017]/SAGA [Defazio et al., 2014]), (d) with/without intercept, (e) one-vs-rest or multinomial for multi-class, (f) with/without class balancing (note that this class balancing operation makes this a two-pass algorithm since we need the first pass to weigh the classes appropriately). We consider a total of 960 hyper-parameter configurations for each experiment.

5. **MLPC.** We consider a multi-layer perceptron trained for a single epoch with the "Adam" stochastic optimization scheme [Kingma and Ba, 2014]. We use `sklearn.neural_network.MLPClassifier` and tune over the following hyper-parameters – (a) number of hidden layers $\{1, 2\}$, (b) number of nodes in each hidden layer $\{16, 64, 128\}$, (b) choice of activation function (ReLU/HyperTangent), (d) regularization, (e) batch size $\in \left[2, 2^8\right]$, (f) initial learning rate $\in \left[10^{-5}, 0.1\right]$ (the rest of the hyper-parameters are left as `scikit-learn` defaults). This leads to a total of 720 hyper-parameters configurations per experiment.

6. **CC.** We also consider a generalization of `CC1` where we classify based on multiple prototypes per class – a test point is assigned the label of its closest prototype. We generate the prototypes per class by k-means clustering (with multiple restarts) and tune over the choice of number of clusters per class in the range $[1, 64]$. This is *not a single pass baseline* but we consider this as a baseline since it is a common compression technique for `k-NNC`.

S3.3 Additional evaluations on synthetic data

Here we present the relative performance of `FBFC` and `FBFC`* for different data dimensionalities in Figure S3.
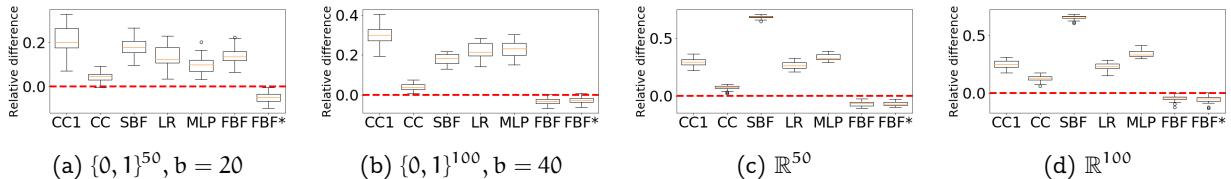

(a) $\{0, 1\}^{50}, b = 20$ (b) $\{0, 1\}^{100}, b = 40$ (c) $\mathbb{R}^{50}$ (d) $\mathbb{R}^{100}$

Figure S3: Performance of `FBFC`/`FBFC`* and baselines relative to the `k-NNC` performance on *synthetic data*. The 10-fold cross-validated accuracy is considered for each of the data sets. The box-plots correspond to the relative difference (*lower is better*) aggregated over 30 repetitions (see text for details). The red dashed line corresponds to matching `k-NNC` performance.

We also study the effect of the number of non-zeros $b < d$ in the binary data on the performance of `FBFC`/`FBFC`* and baselines (Figure S4). The results indicate that, for fixed data dimensionality d, the relative performance of `FBFC` (and variants) is not significantly affected by the choice of $b < d$. `CC` is also robust to changes in b. The performance of `SBFC` seems to improve with increasing b while the opposite behavior is seen for `CC1`, `LR` and `MLPC`.

S3.4 Additional details for OpenML data

We consider two sets of OpenML data sets utilizing the following query for OpenML classification data sets with no categorical and missing features with (i) `min_dim = 11, max_dim = 101, max_rows = 50000`, and (ii) `min_dim = 102, max_dim = 1025, max_rows = 10000`, leading to 79 and 14 data sets respectively where there were no issues with the data retrieval and the processing of the data with `scikit-learn` operators.
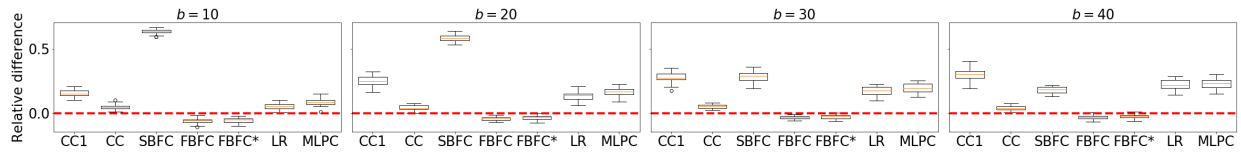**OpenML query for data sets..**

Figure S4: Performance of `FBFC`/`FBFC*` and baselines relative to the performance of k−NNC with varying number of non-zeros b per point for fixed d = 100. All methods undergo a hyper-parameter optimization and the best performance (10-fold cross-validation accuracy) is considered for each of the data sets. The boxplots corresponds to the 30 repetitions (in the form of 30 different synthetic data sets per experimental setting). A relative difference of 0 implies matching the k−NNC (*lower is better*) − the red dashed line corresponds to k−NNC performance.

```python
from openml.datasets import list_datasets, get_dataset
openml_df = list_datasets(output_format='dataframe')
val_dsets = openml_df.query(
    'NumberOfInstancesWithMissingValues == 0 & '
    'NumberOfMissingValues == 0 & '
    'NumberOfClasses > 1 & '
    'NumberOfClasses <= 30 & '
    'NumberOfSymbolicFeatures == 1 & '
    'NumberOfInstances > 999 &'
    'NumberOfFeatures >= min_dim &'
    'NumberOfFeatures <= max_dim &'
    'NumberOfInstances <= max_rows'
)[[
    'name', 'did', 'NumberOfClasses',
    'NumberOfInstances', 'NumberOfFeatures'
]]
```